Nanoscale

RSC Publishing

PAPER

Metal nanoparticle plasmons operating within a quantum lifetime

Cite this: *Nanoscale*, 2013, **5**, 8616

Mehmet Emre Taşgın

We investigate the dynamics of a plasmonic oscillation over a metal nanoparticle when it is strongly coupled to a quantum emitter (*e.g.* quantum dot, molecule). We simulate the density matrix evolution for a simple model, a coupled classical–quantum oscillators system. We show that the lifetime of the plasmonic oscillations can be increased several orders of magnitude, up to the decay time of the quantum emitter. This effect shows itself as the narrowing of the plasmon emission band in the spaser (surface plasmon amplification by the stimulated emission of radiation) experiment [*Nature*, 2009, **460**, 1110], where a gold nanoparticle interacts with the surrounding molecules. Enhancement of the plasmonic excitation lifetime enables stimulated emission to overcome the spontaneous one. The enhancement occurs due to the emergence of a phenomenon analogous to electromagnetically induced transparency (EIT). The effect can find applications in many areas of nanoscale physics, such as in quantum information with plasmons and in increasing solar cell efficiency.

Received 3rd May 2013
Accepted 25th June 2013

DOI: 10.1039/c3nr02270f

www.rsc.org/nanoscale

1 Introduction

Ordinarily, the response of atoms to an electromagnetic field mimics a two-level quantum system since the degeneracy in the excited levels is masked out by dipole selection rules. However, if the dipole allowed excited state is microwave coupled to the forbidden one, the dielectric response will be severely modified.[2] A transparency window emerges at the resonance frequency, where without microwave drive an absorption peak would have been observed. This phenomenon is called Electromagnetically Induced Transparency (EIT). The vanishing absorption is due to the following explanation. The microwave coupling splits the dipole allowed excited state into two (Stark effect[3]). Since the splitting is smaller than the decay rate of the excited level, an optical beam couples the ground state to each of the auxiliary levels. When the two Rabi oscillations are out of phase, the absorption cancels and the atom stays in the ground state.[4–7] The modified absorption is proportional to the decay rate of the dipole forbidden transition (much smaller) instead of the allowed one.[2] EIT-like schemes underlie the physics of ultra-slow light propagation[8,9] and index enhancement.[10]

A similar phenomenon shown in ref. 5–7 takes place for the two coupled classical oscillators (C.O.), where the first one has a high damping rate (low-quality) and the second one has a low damping rate (high-quality). When the low-quality C.O. is driven by a harmonic force, the absorbed power is governed by the damping rate of the high-quality one. Such a phenomenon takes place similarly due to the destructive interference of the two normal modes of the coupled oscillators system.[5,6] In 2009, Soukoulis and colleagues demonstrated the classical analog of EIT in split ring resonators (SRRs).[11,12] They capacitively coupled a dipole (low-quality) SRR to a quadrupole (high-quality) one by closely placing the gaps of the two SRRs. Electromagnetic drive is on the dipolar oscillator, because incident radiation couples only to the dipolar one. The group showed that the response of the dipolar SRR exhibits a dip at the resonance frequency which is 43 THz.

Classical analogs of EIT are shown to have many applications in the field of plasmonic physics. The coupling of dipole and quadrupole plasmonic modes of two rectangular thin plates (or rectangular gaps in metallic plates) manufactured in submicron dimensions are shown to exhibit EIT-like resonances and transparency windows.[13–26] In such devices, slow light propagation,[27,28] electromagnetically induced absorption,[12,21] and anomalous light transmission (where covering the subwavelength nanoaperture with gold nanodisks unexpectedly enhances the light transmission)[29] are observed. The former two effects are proposed to be used in solar cell applications,[30,31] because they trap the light inside solar cell for a longer time and provide enhanced light–matter interaction for pair creation.[30] The lifetime of the quadrupole moment limits the trapping time in solar cells.

Meanwhile, intense research is being conducted on the control of quantum objects (emitters) by coupling them to plasmonic excitations of nanoantennas.[32] The plasmon resonance frequencies of nanoantennas are in the optical range and they are tunable by changing the length/width and manufacturing material of the nanoantennas.[33–39] In 2010, van

Department of Electrical and Electronics Engineering, Kırklareli University, 39020 Karahıdır, Kırklareli, Turkey. E-mail: metasgin@kirklareli.edu.tr; Fax: +90-288-214-0516; Tel: +90-288-214-0514

Hulst and colleagues coupled a quantum dot (QD) to a gold nanoantenna operating at 800 nm.[32] They showed that the QD (excited electronically) transfers the excitation energy[35] to the nano Uda antenna due to the strong coupling and highly directional radiation. Plasmonic nanoparticles enhance the optical cross-section of a QD by five orders of magnitude by localizing the incident light.[40] This gives rise to potential for radiative communication between optical quantum emitters. It is shown that such hybrid systems composed of coupled classical and quantum objects also display Fano-like (or EIT-like[50]) resonances.[40–49] The absorption spectrum of the plasmonic nanoantenna displays a dip due to the destructive interference of the absorption paths.

In this paper, we explore the dynamics of a classical oscillator (plasmonic oscillations on a nanometal) coupled to a quantum emitter (quantum dot,[32,33,35,51,68] nitrogen-vacancy center[36,52,53] or molecule[54]). We show that the lifetime of the classical oscillator lengthens due to the coupling, and it approaches the longer lifetime of the quantum emitter. The model system is a quantum object attached on the nanoantenna to a position where the dipolar mode results in very strong electric field localization (Fig. 1). The localized electric field (five orders larger compared to the incident field[40]) interacts with the quantum emitter. Hence, a dipole–dipole type effective coupling occurs between the antenna and the quantum object.[40–49] Because of the coupling, a transparency window emerges at the center of the absorption spectrum of the antenna, see Fig. 2.

The plasmonic oscillations are driven by a harmonic force which stands for the incident light. The coupled system reaches the steady state in much longer times (see Fig. 6). Thus, nanometal stays polarized for much longer times. Regarding metal nanoparticles, the decay rate of the plasmonic excitations ($\gamma_q \sim 10^{14}$ Hz, or ~100 meV)[40,56] is very large compared to the decay rate of the quantum objects ($\gamma_{eg} \sim 10^9$ Hz, or ~1 μeV for QD[49]). In the coupled system, plasmonic oscillation evolves in time as if it has the tiny decay rate of the quantum emitter.

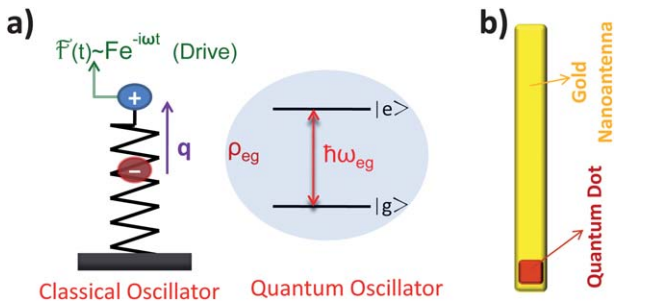

Fig. 1 (a) A classical oscillator driven by an external harmonic source $F(t) = Fe^{-i\omega t}$ is coupled to a quantum oscillator of resonance frequency ω_{eg}. Interaction is of the dipole–dipole type: the dipole induced on the classical oscillator ($\sim q$) is coupled to the quantum one ($\sim \rho_{eg}$). The quantum decay rate (γ_{eg}) is very small compared to the damping (γ_q). (b) The corresponding physical system for the model. A quantum dot is attached over the gold nanoantenna. Plasmonic oscillations on the antenna induces a strong electric field at the ends of the bar. The localized electric field (10^5 times of the incident one[40,55]) couples to the quantum dot. The dipolar excitation of the antenna is driven with the incident optical light.

This effect has already been shown in the spaser experiment by Noginov *et al.*[1,57,58] They demonstrated the stimulated emission of plasmonic excitations in a gold nanoparticle core placed in a dye-doped silica shell. They observed a change in the emission spectrum from a broad band to a narrow line (~10^{12} Hz, or ~1 meV). The narrowing can be explained within our EIT scheme as follows. The gold nanoparticle core couples to the dye molecules more when silica shell is doped more densely. The coupled plasmon–molecule system is governed by the behaviour of the molecular excited level. Thus, the internal conversion rate of the molecule (about ~10^{12} Hz, or ~1 meV) determines the new plasmon emission band, which is narrower. Additionally, by using plasmons with an increased lifetime the stimulated emission can dominate the spontaneous emission rate, as the spaser established.

The presented effect promises many nanoscale applications. Metal nanoparticle covered solar cell surfaces can trap incident solar light for much longer times. As well, such configurations can lead to slower light propagation. Moreover, an increased lifetime enables quantum information processing (including entanglement) with plasmons.

Our simulations also verify a complementary effect. The presence of metal nanoparticles enlarges the decay rate of the quantum emitter,[51–53] see Fig. 7.

The paper is organized as follows. In Section 2.1, we introduce the Hamiltonian for the coupled classical–quantum oscillator system. We drive the equations of motion for the system using density matrix formalism. We include the damping, quantum decay rates and the drive on the C.O. In Section 2.2, we show the emergence of the EIT-like transparency window. At resonance, power absorption from the drive (by the C.O.) is governed by the quantum decay rate (γ_{eg}) instead of C.O. damping (γ_q). In Section 2.3, we adopt an analytical form for the dipolar polarization in the plasmonic mode of the nanoantenna in the vicinity of the resonance. In Section 2.4, we picture the shift of the transparency window to the resonance of the quantum emitter (ω_{eg}), when classical and quantum oscillators are not perfectly tuned. In Section 3, we show that the durations for reaching the steady-state is governed by the lifetime of the quantum object ($1/\gamma_{eg}$) for the coupled system. Thus, plasmons stay polarized for longer times, even if the steady-state value for the polarization may vanish. We also discuss the connection with the spaser experiment[1,57,58] (Section 3.1) and possible solar cell applications (Section 3.2). In Section 3.3, we show that lifetime of the excited quantum emitter is shortened by the plasmon damping. In Section 4, we summarize the paper and discuss the possible applications of the coupled classical-quantum system.

2 Analog of EIT in coupled classical–quantum oscillators system

In this section, we derive the equations of motion for a system where a classical oscillator (C.O.) is strongly coupled to a quantum emitter. The coupling is through the dipole–dipole interaction. Resonance frequencies of the oscillators are in the optical regime. We present the effective Hamiltonian for the

system and derive the equations of motion using the commutation relations. We plot the power absorbed by the C.O. and depict the emergence of a transparency window (no absorption region) about the resonance frequency.

We consider a system where a quantum object (*e.g.* quantum dot, molecule or a nitrogen-vacancy center) is attached over a plasmonic nanoantenna that works in the classical regime[65] (see Fig. 1). The incident light couples to the plasmonic excitation mode of the nanoantenna. The coupling of light to a single quantum emitter is of negligible strength compared to the plasmon. The dipole oscillations, which create a very strong localized electric field over the nanoantenna, couple to the dipolar excitation of the quantum emitter. In Fig. 1b for example, a quantum dot is placed at a position (end of the nanoantenna) where the dipolar plasmon mode gives the maximum electric field. The resultant interaction becomes dipole–dipole type. The effective system is: a quantum object coupled to a C.O. which is driven by an external source. The resonance of the plasmonic mode of the C.O. (ω_q) is tuned (by varying its size) close to the spacing between the ground and excited levels of the quantum oscillator (ω_{eg}). Here, we consider an oversimplified model of the hybrid system. We mainly aim to demonstrate the phenomenon of lifetime enhancement. In more realistic calculations[44,45] one has to consider complicating effects, such as the influence of the dielectric environment.

2.1 Hamiltonian and equations of motion

The total hamiltonian ($\hat{H}$) for such a system can be written as the sum of the energy of the quantum object, energy of the plasmonic oscillations, and the dipole–dipole interactions energy

$$\hat{H}_0 = \omega_e|e\rangle\langle e| + \omega_g|g\rangle\langle g|, \tag{1}$$

$$\hat{H}_q = \frac{\hat{p}^2}{2m} + \frac{1}{2}m\omega_q{}^2\hat{q}^2, \tag{2}$$

$$\hat{H}_{int} = g_c\hat{q}(e^{i\theta}|e\rangle\langle g| + e^{-i\theta}|g\rangle\langle e|), \tag{3}$$

respectively. The dipole moment induced on the antenna (created by the plasmonic oscillations) is proportional to the displacement ($\hat{q}$) of the classical oscillator. The dipole moment of the quantum emitter is proportional to the off-diagonal matrix element ρ_{eg}. In eqn (3), $\hat{q}$ (oscillating with freq. ω_q) couples to the quantum dipole excitation ($e^{i\theta}|e\rangle\langle g| + e^{-i\theta}|g\rangle\langle e|$), where g_c is in units of [freq./length] and $e^{i\theta}$ is the phase of the matrix element. Parameter m is not directly referred to in our derivations, it cancels similarly to the case of quantization of electromagnetic fields (see Chapter 1 in ref. 2).

We use the commutation relations (*e.g.* $i\hbar\dot{\hat{q}} = [\hat{q}, \hat{H}]$) in deriving the equations of motion (EM). We keep $\hat{q}$ quantum up to a step in order to avoid any fault in the EM. After obtaining the dynamics in the quantum approach, we carry $\hat{q}$ to classical ($q(t)$). Using the rotating wave approximation (RWA), the equations take the form

$$\ddot{q}_0(t) + \gamma_q\dot{q}_0(t) + \omega_q{}^2q_0(t) + \frac{\hbar}{m}g_ce^{-i\theta}\rho_{eg}^*(t) = \frac{F}{m}e^{-i\omega t}, \tag{4}$$

$$\dot{\rho}_{eg}(t) = (i\omega_{eg} - \gamma_{eg})\rho_{eg} - ig_ce^{-i\theta}q_0^*(\rho_{ee} - \rho_{gg}), \tag{5}$$

$$\dot{\rho}_{ee}(t) = -\gamma_e\rho_{ee}(t) - ig_c(e^{i\theta}q_0\rho_{eg} - \text{c.c.}), \tag{6}$$

where we use the complex amplitude $q_0(t) \sim e^{-i\omega t}$ for describing oscillations. This is related to the displacement of the C.O. as $q(t) = q_0(t) + q_0^*(t)$. In eqn (4), we introduce the harmonic driving force $\left(\frac{F}{m}e^{-i\omega t}\right)$, of frequency ω, on the plasmonic oscillator. Density matrix elements ρ_{ee}, ρ_{gg}, and ρ_{eg} belong to the quantum emitter. γ_{ee} is the decay rate of the quantum emitter from the excited state to the ground state. The decay rate of the off-diagonal matrix element ρ_{eg} (or the polarization of the quantum emitter) is represented by $\gamma_{eg} = \gamma_{ee}/2$. The damping rate of the classical (plasmonic) oscillator is γ_q. Since γ_{ee} belongs to a quantum object, we have $\gamma_{ee} \gg \gamma_q$. For example, the typical value for the decay rate of a molecular excitation (determined by internal conversion rate) is $\gamma_{ee} \sim 10^{12}$ Hz, whereas the damping rate of plasmonic oscillation is $\gamma_q \sim 10^{14}$ Hz.[56] The constraint on the conservation probability $\rho_{ee} + \rho_{gg} = 1$ accompanies eqn (4–6).

We seek solutions of the form[5,6]

$$q_0(t) = \tilde{q}_0e^{-i\omega t} \text{ and } \rho_{eg}(t) = \tilde{\rho}_{eg}e^{-i\omega t}, \tag{7}$$

for the long term (steady-state) behaviour, where $\tilde{q}_0$ is a complex number and related to the displacement of the C.O. as

$$q(t) = \tilde{q}_0e^{-i\omega t} + \tilde{q}_0e^{i\omega t}. \tag{8}$$

The density matrix element (of amplitude $\tilde{\rho}_{eg}$) oscillates with the source frequency in the steady state. Inserting eqn (7) into eqn (4–6) we obtain the equations

$$(\omega_q{}^2 - \omega^2 - i\gamma_g\omega)\bar{q} + f_c\omega_qe^{-i\theta}\tilde{\rho}_{eg}^* = \bar{F}, \tag{9}$$

$$[i(\omega - \omega_{eg}) + \gamma_{eg}]\tilde{\rho}_{eg} + if_ce^{-i\theta}\bar{q}^*(\rho_{ee} - \rho_{gg}) = 0, \tag{10}$$

$$\gamma_{ee}\rho_{ee} = -if_c(e^{i\theta}\bar{q}\tilde{\rho}_{eg} - e^{-i\theta}\bar{q}^*\tilde{\rho}_{eg}^*), \tag{11}$$

relating the solutions for the slowly varying variables $\bar{q}$, $\tilde{\rho}_{eg}$ and populations ρ_{ee} and ρ_{gg}. We have the additional equation $\rho_{ee} + \rho_{gg} = 1$ for the number (probability) conservation. $\bar{q} = \tilde{q}/a_0$ is the dimensionless (scaled) slowly varying (complex) displacement of the C.O., with $a_0 = (\hbar/m\omega_q)^{1/2}$ as the characteristic oscillator length. $f_c = g_ca_0$ is the coupling frequency (strength) and $\bar{F} = F/ma_0$ is the scaled force, in units of [freq.]^2. We note that, in eqn (10), scaling results to $\frac{\hbar}{m}\frac{g_c}{a_0} = \frac{\hbar}{m}\frac{g_ca_0}{a_0{}^2} = g_c\omega_q$. Therefore, we do not refer to mass m any more.

2.2 Transparency window in absorption spectra

We solve the set of nonlinear eqn (9–11) and we obtain the response of the coupled classical–quantum oscillators system to a driving harmonic field (force). In the solutions, we make the

assumption that driving force ($\bar{F}e^{-i\omega t}$) has always been on (until $t = -\infty$), implicitly.

Regarding the plasmonic oscillations, $q(t) = \tilde{q}_0 e^{-i\omega t} + \tilde{q}_0 e^{i\omega t}$ corresponds to dipolar polarization on the antenna. Thus, the real/imaginary part of $\tilde{q}_0$ refers to the polarization/absorption. This is analogous to the relation $\boldsymbol{P}_\omega = \chi(\omega)\boldsymbol{E}_\omega$, where $\boldsymbol{P}$, $\boldsymbol{E}$, and χ stand for the polarization, electric field, and dielectric susceptibility, respectively. An equivalent relation can be calculated also from the power that force exerts on the oscillator (force × velocity)[5,6] per cycle,

$$P(t) = \mathrm{Re}\{-i\omega F\tilde{q}\} = \mathrm{Im}\{\omega F\tilde{q}\}. \quad (12)$$

Therefore, the absorbed power is proportional to the imaginary part of the $\tilde{q}$, as discussed above. In Fig. 2, we have plotted the absorbed power for varying drive (source) frequency ω. We took the resonance frequency of the plasmonic mode as equal to the quantum level spacing, *i.e.* $\omega_{eg} = \omega_q$. When the C.O. is not coupled with the quantum object, the absorption shows a peak at the resonance $\omega = \omega_q$ (dashed-line in Fig. 2). On the other hand, if the C.O. is coupled to the Q.O. with coupling strength $f_c = 0.1\omega_q$, the emergence of a transparency window at the center of the absorption peak ($\omega = \omega_q$) is observed (solid-line in Fig. 2). In the vicinity of $\omega = \omega_q$, the absorbance is proportional to the quantum decay rate γ_{eg} instead of the classical one γ_q, similar to ref. 2, 5 and 6 (see eqn (18) below). The driving force is $\bar{F} = 0.01$ in units of $\omega_q{}^2$, and corresponds to a pump intensity of about 10^3 mW cm^{-2}.

Regarding plasmonic oscillations, $q(t)$ corresponds to the polarization field in the antenna. So, in Fig. 3, we have plotted the nanoantenna polarization $\mathrm{Re}\{\bar{q}\}$ (solid-line) together with the antenna absorption ($\mathrm{Im}\{\bar{q}\}$). Fig. 3 depicts the common form of the EIT-like response.[2]

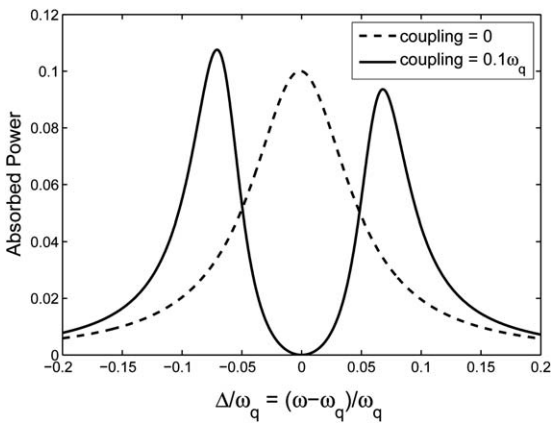

Fig. 2 The power classical oscillator (nanoantenna) absorbs from the driving force (electromagnetic field). When the nanoantenna operates alone absorption is peaked (dashed-line) about the resonance frequency of the antenna (ω_q). If the nanoantenna is coupled to a quantum oscillator (*e.g.* quantum dot) a transparency window occurs (solid-line) in the mid of the absorption peak. The new absorption at the resonance is determined by the decay rate of the quantum dot ($\gamma_{eg} \sim 10^9$ Hz), which is several orders of magnitude smaller compared to the damping ($\gamma_q \sim 10^{14}$ Hz). The quantum level spacing is perfectly tuned with the resonance of the antenna, *e.g.* $\omega_{eg} = \omega_q$. The damping and quantum decay rates $\gamma_q = 0.1\omega_q$ and $\gamma_{eg} = 0.5 \times 10^{-4}\omega_q$ are used in the simulation. The scaled driving force is $\bar{F} = 0.01$ (in units of $\omega_q{}^2$).

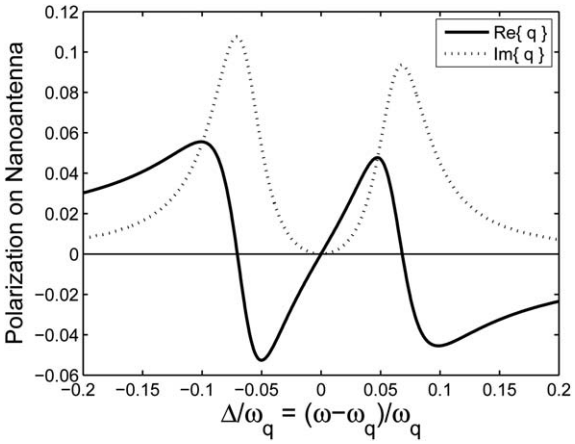

Fig. 3 The real (solid-line) and the imaginary (dotted-line) parts of the displacement ($\bar{q}$) of the classical oscillator. The real part corresponds to the polarization induced on the nanoantenna. The imaginary part is proportional to the antenna absorption. We clearly observe the EIT-like behaviour.[2,5,6,11,12] The parameters are the same as in Fig. 2.

Fig. 4 plots the corresponding values for the polarization in the quantum dot ($\bar{\rho}_{eg}(\omega)$) and the excitation fraction ($\rho_{ee}(\omega)$). We see that (solid-line in Fig. 4b) the quantum dot stays polarized ($\mathrm{Re}\{\rho_{eg}\} \neq 0$) without absorption ($\mathrm{Im}\{\rho_{eg}\} = 0$) at resonant drive $\omega = \omega_q$. In addition, the quantum dot becomes partially excited ($\rho_{ee} \neq 0$) about the resonance. The reason for the asymmetric absorption peaks in Fig. 2 is due to the antisymmetric absorption profile (about $\Delta = 0$) of the quantum oscillator. For $\omega > \omega_q$, the quantum object displays gain ($\mathrm{Im}\{\rho_{eg}\} < 0$) in the coupled system. Such asymmetric absorption (scattering) profiles are common to Fano resonances.[24]

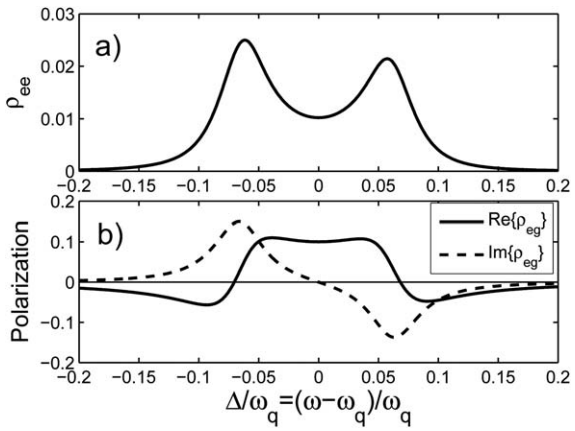

Fig. 4 The corresponding steady state values for the (a) excitation fraction and (b) polarization in the quantum emitter, which is coupled to the nanoantenna (classical oscillator). At resonance, the quantum emitter stays polarized ($\mathrm{Re}\{\rho_{eg}\} \neq 0$) with a finite excitation probability ($\rho_{ee} \neq 0$). The absorption of the quantum object vanishes at resonance ($\mathrm{Im}\{\rho_{eg}\} = 0$).

2.3 Analytical form for antenna polarization ($\bar{q}$)

Exact expressions for $\bar{q}$ are cumbersome since they include the solutions of the cubic equations. However, analytical expressions where the solution for the population inversion $y = \rho_{ee} - \rho_{gg}$ left implicit give us clues about the response of the coupled system. When the expression for ρ_{eg}, obtained from eqn (9), is used in eqn (10), one obtains

$$\bar{q} = \bar{F}\,\frac{(\omega - \omega_{eg}) + i\gamma_{eg}}{D_R + iD_I}, \tag{13}$$

where

$$D_R = (\omega - \omega_{eg})({\omega_q}^2 - \omega^2) + \gamma_q\gamma_{eg}\omega - {f_c}^2\omega_q y \tag{14}$$

$$D_I = \gamma_{eg}({\omega_q}^2 - \omega^2) - \gamma_q\omega(\omega - \omega_{eg}) \tag{15}$$

are the real and imaginary parts of the denominator in eqn (13). $\bar{F}$ is the scaled force in units of [freq.]^2. The value of population inversion y is determined by solving the cubic equation

$$\frac{1+y}{2} = -\frac{{f_c}^2 y}{(\omega - \omega_{eg}) + {\gamma_{eg}}^2}|\bar{q}|^2, \tag{16}$$

which is obtained by using the expression for ρ_{eg} in eqn (11). From eqn (16) it can be seen that $y < 0$ must be satisfied. Among the three roots for y, only one is real or satisfies all of the eqn (9–11).[66]

When $\omega = \omega_q = \omega_{eg}$, eqn (13) simplifies to

$$\bar{q} = i\,\frac{\bar{F}\gamma_{eg}}{(\gamma_q\gamma_{eg} - {f_c}^2 y)\omega_q}, \tag{17}$$

which is purely imaginary and results in no polarization. Since γ_{eg} is very small compared to all frequencies, absorption is represented by

$$P \simeq \bar{F}\gamma_{eg}/(-{f_c}^2 y) \tag{18}$$

which is proportional to γ_{eg}, not γ_q.[5,6] This simple result depicts the expected absorption cancellation effect common to the EIT response. For $\omega = \omega_q = \omega_{eg}$ and $\gamma_{eg} \to 0$, the equation for y [that is eqn (16)] simplifies to

$$y^2 + y + c = 0, \tag{19}$$

where $c = 2\bar{F}^2/{f_c}^2{\omega_q}^2$. Eqn (19) has real solutions only if the discriminant is nonnegative, that is if $\bar{F} < (f_c\omega_q/2\sqrt{2})$. Hence, in the linear regime (when drive is small) y has the real solutions

$$y_{1,2} \simeq -\frac{1}{2} \pm \frac{(1-4c)^{1/2}}{2}. \tag{20}$$

In our simulations, we verify that eqn (17), (18) and (20) describe the absorption in the steady state – for resonantly matched classical, quantum oscillators with the source – provided that γ_{eg} is small compared to other frequencies.

2.4 Shift of the transparency window when C.O. is not perfectly tuned to Q.O. ($\omega_{eg} \neq \omega_q$)

When the resonance frequency of the dipole mode of the plasmonic excitation of the nanoantenna does not match the quantum level separation (ω_{eg}), the behavior of the EIT-like response is modified. The position, where EIT occurs shifts to $\omega \simeq \omega_{eg}$ (see Fig. 5). This takes place due to the following effect. The spectral width of the quantum oscillator (quantum dot) $\Delta_{qua} \simeq \gamma_{eg} = 0.001\omega_q$ is very tight compared to the spectral width of the C.O. $\Delta_{cls} = 0.1\gamma_q$. Thus, in order to establish the coupling, C.O. rearranges its frequency (within $\Delta_q \sim \gamma_q$) in order to match the energy spacing of the quantum system.

3 Enhanced duration for plasmonic oscillations

In Fig. 6, we have plotted time evolutions of the antenna polarization ($\bar{q} = \mathrm{Re}\{\bar{q}\} + i\mathrm{Im}\{\bar{q}\}$) when there is no coupling (Fig. 6a) between the classical–quantum oscillators and in the existence of coupling $f_c = 0.1\omega_q$ (Fig. 6b). Quantum level separation is $\omega_{eg} = 1.01\omega_q$, decay rates are $\gamma_q = 0.1\omega_q$ and $\gamma_{eg} = 0.0005\omega_q$. We observe that the coupled oscillator reaches the steady state in the order of $\gamma_q/\gamma_{eg} \sim 200$ times longer compared to the uncoupled one. Thus, the coupled system remains polarized for a much longer time, even if the final polarization for both cases may be zero at the steady state (not zero in Fig. 6b).

In this paper, we aim to present simply the possibility of the lifetime enhancement for a C.O. (plasmonic field) without concentrating on the specific system parameters. Even though the typical frequency values for nanoantenna plasmons can be specified, the damping rates for quantum emitters occupy a wide range. The surface plasmon frequencies for metal nanoparticles are in the optical range $\omega_q \sim 10^{15}$ Hz (or ~1 eV). The typical decay rate for plasmons is $\gamma_q \sim 10^{14}$ Hz.[40,56] On the other hand, the decay rate for quantum objects varies. An alkali atom can have $\gamma_q \sim 10^7$ Hz. The typical value for a QD is about $\gamma_q \sim 10^9$ Hz.[49] In dye molecules, even though the radiative

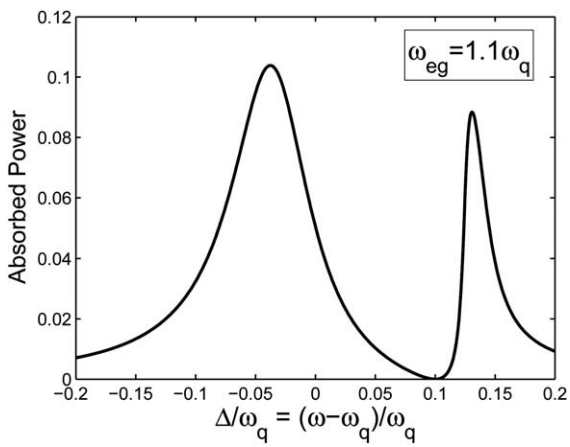

Fig. 5 The spectral variation of the absorbed power on the nanoantenna when the resonance frequency of the antenna (ω_q) is not perfectly tuned to the quantum level spacing (ω_{eg}). The position, where the EIT-like response occurs, shifts to the quantum resonance $\omega = \omega_{eg} = 1.1\omega_q$. The antenna can rearrange its operation frequency within its spectral width $\pm\gamma_q = \pm 0.1\omega_q$ in order to match the quantum oscillation. The coupling strength is $f_c = 0.1\omega_q$ and the scaled driving force is $\bar{F} = 0.01$ (in units of ${\omega_q}^2$).

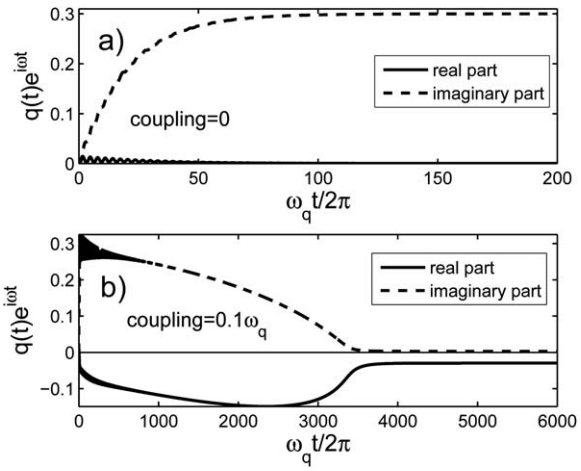

Fig. 6 Comparison of the duration for the two systems to reach the steady-state polarization. The C.O. is driven by the harmonic force $F(t) = Fe^{-i\omega t}$. (a) The nanoantenna (C.O.) is not coupled to the quantum emitter (*e.g.* a molecule). Antenna polarization (Re{q}) reaches the steady-state at about $\omega_q t = 2\pi \times 20$. (b) The nanoantenna is coupled to the quantum dot with a coupling strength $f_c = 0.1\omega_q$. The antenna reaches the steady-state in about $\omega_q t = 2\pi \times 4000$. Coupled nanoantenna stay polarized for about $\gamma_q/\gamma_{eg} \simeq 200$ times longer compared to the uncoupled one. Lifetime enhancement in plasmon excitations enables the use of metal nanoparticles in plasmonic quantum information and in solar cell applications.[30,31,59,60] Quantum level spacing is $\omega_{eg} = 1.01\omega_q$. Decay rates are $\gamma_q = 0.1\omega_q$ and $\gamma_{eg} = 0.0005\omega_q$. The driving force is $\bar{F} = 0.03$ (in units of ω_q^2) and the drive frequency is $\omega = \omega_q$. The parameters correspond to the spaser experiment.[1,57,58]

lifetime is as long as nanoseconds, the internal conversion rate ($\gamma_q \sim 10^{12}$ Hz) determines the duration of the excitation.

3.1 The spaser experiment

The scaled values in Fig. 6 correspond to a plasmon–molecule coupled system with frequencies $\omega_q \sim 10^{15}$ Hz, $\gamma_q \sim 10^{14}$ Hz and $\gamma_{ee} \sim 10^{12}$ Hz ($\gamma_{eg} = \gamma_{ee}/2$). The coupling frequency $f_c = \gamma_q$ may be varied by closer placing the molecule–nanoparticle system. Such strong coupling regimes ($f_c > \gamma_q$) are achievable.[69] This system has been experimented with by Noginov *et al.*[1,57,58] within the spaser (surface plasmon amplification by stimulated emission of radiation) concept. For stronger coupling between the molecule-doped silica shell and gold nanoparticle core – by increasing the doping concentration – a narrower emission band for the combined system can be observed. Decreasing the spontaneous emission rate (plasmon decay rate) above a critical pump stimulated emission of plasmons wins against the spontaneous one.

It is natural to expect the emergence of the lifetime enhancement effect after a sufficient driving force (pump intensity). The induced dipole field must be high enough for the coupling energy to be of a similar order as the plasmon decay rate. Because, the energy transfer rate from plasmon excitation to the quantum emitter must be not negligible compared to the energy transfer rate to the vacuum modes.

Noginov *et al.* point out that when the density of the hybrid nanoparticles is decreased (not the damping concentration for a single nanoparticle), the emission intensity decreases but the narrowing in the emission spectrum is preserved. This shows that, spectral narrowing originates from a single hybrid system above a critical doping (molecule) concentration. Thus, lasing originates, not from the collective act of the ensemble of the hybrid systems, but rather originates from the extension of the plasmon lifetime in a single system due to the stronger molecule–plasmon coupling.

In order to observe the duration enhancement for the plasmonic oscillation (polarization) one does not need a perfect matching between the plasmon resonance frequency and the quantum level spacing. In Fig. 5, we observe that position of the EIT center is determined by the quantum emitter.

A similar lifetime enhancement effect occurs when a dipolar plasmon mode is coupled to a high-life quadrupole plasmon mode, a full classical analog of EIT.[30,31,59,60] However, the lifetime for a quantum excitation is much longer than the classical quadrupole plasmon one.

3.2 Nanoscale applications

The common aim in solar cell research is to increase the time that sunlight spends in/on the semiconductor panels.[27,28,30,31,59,60] The incident sun light is trapped in the silver/gold nanospheres (of diameter 80 nm) which are placed on the surface of the solar cells by the de-wetting technique.[30,59,60]

In a coupled metal nanosphere–quantum emitter system, light trapping duration can be extended up to 10^{-9} s (for certain drive frequencies) using quantum dots (QDs). This increases the pair formation efficiency in solar panels. In ref. 54, the self-assembled manufacturing of bio-molecules that are coupled to gold nanospheres was reported. Random distributions of such objects on the solar cell surface is possible to work as EIT centers. Alternatively, sputtering molecules over the surface can be expected to work. Using molecules with different quantum level spacings, EIT centers can cover different frequency ranges. A variety of molecules can be fit into a wavelength square. Even though QDs display higher lifetimes, they are not appropriate for self-assembled (mass production) techniques.

On the other hand, QDs can be used in quantum information processing. Plasmons (of high electromagnetic cross section) with increased lifetime can be utilized in processes which need quantum entanglement.

3.3 Shortened decay time for quantum emitters

We additionally verify a complementary effect that the decay time of the electronically excited quantum emitter to the ground state is shortened due to the presence of the metal nanoparticles.[51–53] In Fig. 7, the quantum dot is prepared initially in the excited state ($\rho_{ee} = 1$). There exists no drive, but the quantum dot is coupled with a strength of $f_c = 0.1\omega_q$ to the nanoantenna. Comparing Fig. 7a and b, the coupled composite system emits the energy in a much shorter time (about 10 times).

The increased quantum decay rate can also be attributed to the change in the density of states due to the hybridization of the quantum dot and the nanometal[53] (Purcell effect). Here, we observe a parallel effect due to the modification of the effective decay rate of the quantum emitter by the damping rate of the plasmonic antenna. This effect has totally different origins.

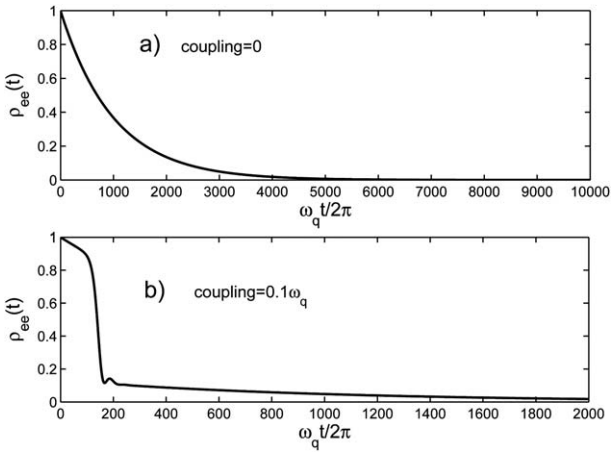

Fig. 7 Comparison of the durations for the excited quantum emitter to decay into the ground state. The quantum emitter is prepared initially in the excited state ($\rho_{ee} = 1$) and there is no applied drive. (a) Quantum dot is not coupled to nanometal. Decay to ground state happens in the natural decay time $1/\gamma_{eg} \sim 2000$. (b) Quantum dot is coupled to the metal nanoantenna with strength $f_c = 0.1\omega_q$. The decay of the composite system takes only $\sim 200/\omega_q$ time. Quantum level spacing is $\omega_{eg} = 1.01\omega_q$. Decay rates are $\gamma_q = 0.1\omega_q$ and $\gamma_{eg} = 0.0005\omega_q$.

Therefore, the observed shortening has dual origins both working in the same direction (shortening).

4 Summary and conclusions

Incident sunlight couples very strongly to the metal nanoparticle plasmons. The trapped intense radiation results in enhanced light–matters interaction.[30] However, these oscillations last only about $1/\gamma_q \sim 10^{-14}$ s and the light is re-radiated in different frequencies (heat). We show that the lifetime of the light trapping in plasmonic oscillations can be increased up to the quantum decay time $1/\gamma_{eg} \sim 10^{-9}$ s. The dynamics of the driven plasmons is governed by the lifetime of the quantum emitter (see Fig. 6) which is coupled to it. The new lifetime is limited with the coherence time of the driving source.[61,62]

The effect is observed in the experiment[1,57,58] demonstrating the stimulated emission of plasmon excitations (spaser). The emission band of the coupled metal nanoparticle–molecule system is determined by the internal conversion rate of the dye molecule.

The presence of such an effect is due to the semiquantum–semiclassical analog of electromagnetically induced transparency (EIT).[2] The coupling of the quantum object creates an additional oscillation mode whose frequency is within the uncertainty window (proportional to the damping rate) of the classical oscillator. The two normal modes of the classical oscillator interfere destructively and absorption cancels. A transparency window emerges at the center of the absorption peak of the plasmonic nanometal. A similar version of duration enhancement also occurs in the full-classical analog of EIT,[5,6,11] where a dipole mode is coupled to a high-life quadrupole mode.[12,59,60] However, the lifetime of quantum excitation is very large compared to the quadrupole mode plasmon lifetime.

The EIT in coupled classical–quantum systems enables us to benefit from useful features of both systems. In such a device, one can combine the large interaction cross section of plasmons (with light) and long decay time of the quantum object. This allows one to use nanoantennas in quantum information. Such an effect can also be adopted in solar cell applications for the longer trapping of light.

In addition, the slow light propagation occurring within the transparency window lasts much longer. Regarding the macroscopic light propagation inside the solar cell, this effect additionally increases the optical path length.

Acknowledgements

I acknowledge support from TÜBİTAK-KARİYER Grant no. 112T927 and TÜBİTAK-1001 Grant no. 110T876. I specially thank Gürsoy B. Akgüç for guiding discussions and his intensive help with the manuscript. I specially thank T. Çetin Akıncı and Serhat Şeker for their motivational support.

Notes and references

1 M. A. Noginov, G. Zhu, A. M. Belgrave, R. Bakker, V. M. Shalaev, E. E. Narimanov, S. Stout, E. Herz, T. Suteewong and U. Wiesner, *Nature*, 2009, **490**, 1110.
2 M. O. Scully and M. S. Zubairy, *Quantum Optics*, Cambridge University Press, Cambridge, 1997.
3 W. Voigt, *Ann. Phys.*, 1901, **4**, 197.
4 S. E. Harris and J. J. Macklin, *Phys. Rev. A: At., Mol., Opt. Phys.*, 1989, **40**, 4135.
5 C. L. G. Alzar, M. A. G. Martinez and P. Nussenzveig, *Am. J. Phys.*, 2002, **70**, 37.
6 C. L. Garrido Alzar, M. A. G. Martinez and P. Nussenzveig, arXiv:quant-ph/0107061v1, 2001.
7 A. G. Litvak and M. D. Tokman, *Phys. Rev. Lett.*, 2002, **88**, 095003.
8 T. F. Krauss, *Nat. Photonics*, 2008, **2**, 448.
9 M. F. Yanik and S. Fan, *Phys. Rev. Lett.*, 2004, **92**, 083901.
10 M. Fleischhauer, C. H. Keitel, M. O. Scully, C. Su, T. Ulrich and S.-Y. Zhu, *Phys. Rev. A: At., Mol., Opt. Phys.*, 1992, **46**, 1468.
11 P. Tassin, Lei. Zhang, Th. Koschny, E. N. Economou and C. M. Soukoulis, *Phys. Rev. Lett.*, 2009, **102**, 053901.
12 P. Tassin, L. Zhang, L. Zhao, A. Jain, Th. Koschny and C. M. Soukoulis, *Phys. Rev. Lett.*, 2012, **109**, 187401.
13 N. Liu, L. Langguth, T. Weiss, J. Kästel, M. Fleischhauer, T. Pfau and H. Giessen, *Nat. Mater.*, 2009, **8**, 758.
14 X. Liu, J. Gu, R. Singh, Y. Ma, J. Zhu, Z. Tian, M. He, J. Han and W. Zhang, *Appl. Phys. Lett.*, 2012, **100**, 131101.
15 B. Lukyanchuk, N. I. Zheludev, S. A. Maier, N. J. Halas, P. Nordlander, H. Giessen and C. T. Chong, *Nat. Mater.*, 2010, **9**, 707.
16 R. D. Kekatpure, E. S. Barnard, W. Cai and M. L. Brongersma, *Phys. Rev. Lett.*, 2010, **104**, 243902.
17 A. Artar, A. A. Yanik and H. Altug, *Nano Lett.*, 2011, **11**, 1685.

18 A. E. Çetin, A. Artar, M. Turkmen, A. A. Yanik and H. Altug, *Opt. Express*, 2011, **19**, 22607.

19 Z. Ye, S. Zhang, Y. Wang, Y.-S. Park, T. Zentgraf, G. Bartal, X. Yin and X. Zhang, *Phys. Rev. B: Condens. Matter Mater. Phys.*, 2012, **86**, 155148.

20 N. Liu, T. Weiss, M. Mesch, L. Langguth, U. Eigenthaler, M. Hirscher, C. Sönnichsen and H. Giessen, *Nano Lett.*, 2010, **10**, 1103.

21 R. Taubert, M. Hentschel, J. Kaästel and H. Giessen, *Nano Lett.*, 2012, **12**, 1367.

22 N. Papasimakis, V. A. Fedotov, N. I. Zheludev and S. L. Prosvirnin, *Phys. Rev. Lett.*, 2008, **101**, 253903.

23 J. Chen, Z. Li, S. Yue, J. Xiao and Q. Gong, *Nano Lett.*, 2012, **12**, 2494.

24 A. E. Miroshnichenko, S. Flach and Y. S. Kivshar, *Rev. Mod. Phys.*, 2010, **82**, 2257.

25 S. Longhi, *Phys. Rev. A: At., Mol., Opt. Phys.*, 2009, **79**, 023811.

26 C. Zheng, X. Jiang, S. Hua, L. Chang, G. Li, H. Fan and M. Xiao, *Opt. Express*, 2012, **20**, 18319.

27 Y. Huang, C. Min and G. Verosnis, *Appl. Phys. Lett.*, 2011, **99**, 143117.

28 C. Wu, A. B. Khanikaev and G. Shvets, *Phys. Rev. Lett.*, 2011, **106**, 107403.

29 K. Imura, K. Ueno, H. Misawa and H. Okamoto, *Nano Lett.*, 2011, **11**, 960.

30 H. A. Atwater and A. Polman, *Nat. Mater.*, 2010, **9**, 205.

31 J.-L. Wu, F.-C. Chen, Y.-S. Hsiao, F.-C. Chien, P. Chen, C.-H. Kuo, M. H. Huang and C.-S. Hsu, *ACS Nano*, 2011, **5**, 959.

32 A. G. Curto, G. Volpe, T. H. Taminiau, M. P. Kreuzer, R. Quidant and N. F. van Hulst, *Science*, 2010, **329**, 930.

33 N. Livneh, A. Strauss, I. Schwarz, I. Rosenberg, A. Zimran, S. Yochelis, G. Chen, U. Banin, Y. Paltiel and R. Rapaport, *Nano Lett.*, 2011, **11**, 1630.

34 P. Mühlschlegel, H.-J. Eisler, O. J. F. Martin, B. Hecht and D. W. Pohl, *Science*, 2005, **308**, 1607.

35 J. N. Farahani, D. W. Pohl, H.-J. Eisler and B. Hecht, *Phys. Rev. Lett.*, 2005, **95**, 017402.

36 A. W. Schell, G. Kewes, T. Hanke, A. Leitenstorfer, R. Bratschitsch, O. Benson and T. Aichele, *Opt. Express*, 2011, **19**, 7914.

37 I. S. Maksymov, I. Staude, A. E. Miroshnichenko and Y. S. Kivshar, *J. Nanophotonics*, 2012, **1**, 65.

38 P. Biagioni, J.-S. Huang and B. Hecht, *Rep. Prog. Phys.*, 2012, **75**, 024402.

39 R. Esteban, A. G. Borisov, P. Nordlander and J. Aizpurua, *Nat. Commun.*, 2012, **3**, 825.

40 X. Wu, S. K. Gray and M. Pelton, *Opt. Express*, 2010, **18**, 23633.

41 A. Manjavacas, F. J. Garcia de Abajo and P. Nordlander, *Nano Lett.*, 2011, **11**, 2318.

42 P. Weis, J. L. Garcia-Pomar, R. Beigang and M. Rahm, *Opt. Express*, 2011, **19**, 23573.

43 S. G. Kosionis, A. F. Terzis, S. M. Sadeghi and E. Paspalakis, *J. Phys.: Condens. Matter*, 2013, **25**, 045304.

44 R. D. Artuso and G. W. Bryant, *Phys. Rev. B: Condens. Matter Mater. Phys.*, 2010, **82**, 195419.

45 R. D. Artuso and G. W. Bryant, *Nano Lett.*, 2008, **8**, 2106.

46 E. Waks and D. Sridharan, *Phys. Rev. A: At., Mol., Opt. Phys.*, 2010, **82**, 043845.

47 A. Ridolfo, O. Di Stefano, N. Fina, R. Saija and S. Savasta, *Phys. Rev. Lett.*, 2010, **105**, 263601.

48 W. Zhang, A. O. Govorov and G. W. Bryant, *Phys. Rev. Lett.*, 2006, **97**, 146804.

49 S. G. Kosionis, A. F. Terzis, V. Yannopapas and E. Paspalakis, *J. Phys. Chem. C*, 2012, **116**, 23663.

50 EIT and Fano resonances are two specific names for the common phenomenon of absorption (scattering) modification in quantum systems. The name Fano is used when the introduced third level is in the continuous (unbound) spectrum.[25,26] The name EIT is used for quantum systems with the third level is a discrete (nonradiative) quantum level.[2] For the system we study here, the name EIT is more appropriate since we are not dealing with coupling to the continuous spectrum of the quantum or hybrid system.

51 M. Pfeiffer, K. Lindfors, C. Wolpert, P. Atkinson, M. Benyoucef, A. Rastelli, O. G. Schmidt, H. Giessen and M. Lippitz, *Nano Lett.*, 2010, **10**, 4555.

52 L. Zhao, T. Ming, H. Chen, *et al.*, *Nanoscale*, 2011, **3**, 3849.

53 P. Anger, P. Bharadwaj and L. Novotny, *Phys. Rev. Lett.*, 2006, **96**, 113002.

54 S. J. Barrow, X. Wei, J. S. Baldauf, A. M. Funston and P. Mulvaney, *Nat. Commun.*, 2012, **3**, 1275.

55 M. I. Stockman, *Opt. Express*, 2011, **19**, 22029.

56 J. Lehmann, M. Merschdorf, W. Pfeiffer, A. Thon, S. Voll and G. Gerber, *Phys. Rev. Lett.*, 2010, **85**, 2921.

57 D. J. Bergman and M. I. Stockman, *Phys. Rev. Lett.*, 2003, **90**, 027402.

58 D. Li and M. I. Stockman, *Phys. Rev. Lett.*, 2013, **110**, 106803.

59 R. Y. Zhang, B. Shao, J. R. Dong, K. Huang, Y. M. Zhao, S. Z. Yu and H. Yang, *Opt. Mater. Express*, 2012, **2**, 173.

60 M. C. Günendi, İ. Tanyeli, G. B. Akgüç, A. Bek, R. Turan and O. Gülseren, *Opt. Express*, 2013, **21**, 18344–18353.

61 The phase of the sunlight exhibit random fluctuations. This effect has second quantized origin (see Chapter 14.5 in ref. 2, 63 and 64) and gives rise to a finite coherence time ($\tau \sim 10^{-8}$ s) for the incident sun light. For this reason, at the end of each phase-coherence period, one shall consider a reset source. The shift in the oscillation phase of the source can interfere destructively with the previous polarization constructed on the nanometal. Thus, plasmonic and quantum oscillations are reorganized after each phase-coherence period.

62 L. Mandel and E. Wolf, *Optical Coherence and Quantum Optics*, Cambridge University Press, Cambridge, 1995.

63 W. Li, A. K. Tuchman, H.-C. Chien and M. A. Kasevich, *Phys. Rev. Lett.*, 2007, **98**, 040402.

64 G.-B. Jo, Y. Shin, S. Will, T. A. Pasquini, M. Saba, W. Ketterle, D. E. Pritchard, M. Vengalattore and M. Prentiss, *Phys. Rev. Lett.*, 2007, **98**, 030407.

65 Such oscillators can be modelled in the classical regime using Maxwell equations.[12]
66 Near the resonance $\omega = \omega_q = \omega_{eg}$, there occurs a second real root for y. The system of equations we study is nonlinear. Thus, convergence to one of the steady states depends on the initial value.[67] We check that; for the initial conditions $\rho_{gg}(t = 0) = 1$, $\rho_{gg}(t = 0) = 0$ and $q(t = 0) = 0$, real-time simulations of eqn (4–6) converges to the plotted results.
67 S. H. Strogatz, *Nonlinear Dynamics and Chaos*, Perseus Books Publishing L.L.C, New York, 2003.
68 D. Pacifici, H. Lezec and H. A. Atwater, *Nat. Photonics*, 2007, **1**, 402.
69 L. Wang and W. Tan, *Nano Lett.*, 2006, **6**, 84.